Semiconductor Science
and Technology

PAPER

Influence of low-temperature annealing on Schottky barrier height and surface electrical properties of semi-insulating CdTe

To cite this article: M Rejhon *et al* 2017 *Semicond. Sci. Technol.* **32** 085007

IOP Publishing Semiconductor Science and Technology
Semicond. Sci. Technol. **32** (2017) 085007 (6pp) https://doi.org/10.1088/1361-6641/aa7500

Influence of low-temperature annealing on Schottky barrier height and surface electrical properties of semi-insulating CdTe

M Rejhon, J Franc, J Zázvorka, V Dědič and J Kunc

Institute of Physics of Charles University, Faculty of Physics and Mathematics, Charles University, Prague, Czechia

E-mail: rejhonm@karlov.mff.cuni.cz

Received 5 April 2017, revised 11 May 2017
Accepted for publication 25 May 2017
Published 12 July 2017

Abstract

We investigated the influence of low-temperature annealing in ambient air on the fundamental properties of semi-insulating CdTe doped with In and Cl in planar configuration, with gold and indium contacts prepared by evaporation at temperatures up to 373 K. The Au contact was formed by a central electrode and a guard ring, which allows us to separate bulk and surface leakage currents. We measured I–V characteristics and ellipsometry after each annealing step at room temperature. We determined that the change of the Schottky barrier height is responsible for the change of the bulk current, while the surface leakage current is affected by TeO_2 layer thickness.

Keywords: CdTe, low-temperature annealing, Schottky barrier height, TeO_2, bulk and surface leakage current

(Some figures may appear in colour only in the online journal)

1. Introduction

In the last decade, significant research efforts have focused on the material development of CdTe and CdZnTe, which have become materials of choice in applications such as room-temperature spectroscopic x-ray and gamma-ray semiconductor detectors. These materials have optimal operable properties from the viewpoint of direct conversion efficiency of incoming radiation by photoelectric effect (high average atomic number $Z \sim 50$). It is technologically possible to prepare the material as semi-insulating with resistivity 10^9–10^{10} Ω cm by the process of compensation with shallow donors. Furthermore, the signal-to-noise ratio at room temperature can be kept low due to a relatively high bandgap $E_g(300\ \mathrm{K}) \approx 1.53$ eV [1]. The final properties of the detector-grade material are a result of a delicate balance between shallow and deep defects. Relatively small changes of external conditions, especially temperature, can result in substantial modification of trapping and recombination kinetics of free carriers that can be detrimental to charge collection. These changes can be caused not only by standard temperature dependence of trapping and de-trapping of carriers to and from deep levels, but also by thermally induced modifications of surfaces, metal/semiconductor interfaces, and defects in the bulk.

Low-temperature annealing performed typically in the temperature range of 373–523 K, as well as its impact on properties of CdTe-based materials and detectors, has been investigated with controversial results so far. While Wang *et al* [2, 3] and Chattopadhyay *et al* [4] reported increase of leakage currents accompanied by deteriorated detection parameters, other authors observed decrease of leakage currents [5–8]. Kim *et al* [7] studied the influence of the low-temperature annealing in air/vacuum on In/CdZnTe/Au samples with a chemical gold contact and with a gold contact formed by evaporation. They showed that the current decreased after the low-temperature annealing (390− 410 K) in air on the sample with the chemical gold contact due to an oxide layer creation below the gold contact. The same effect was shown by Mergui *et al* [8], who measured the effect of annealing in air on an Au/CdTe interface. He observed that oxide penetrates under the contact and leads to a larger barrier

height, which can explain the decrease of the leakage current. Kim also measured ^{241} Am gamma spectrum before and after low-temperature annealing, and showed a worsening of the FWHM from 10% to 12%. On the other hand, Park [6] showed that the FWHM is the same before and after low-temperature annealing at about 100° C for 8 hours. Both used the planar detector configuration, so they did not distinguish the bulk and surface leakage currents, which in turn could affect the gamma spectra resolution. Pekárek *et al* measured the passivation influence on detector performance and showed improvement in both the resolution and charge-collection efficiency with lower surface leakage current [9]. However, the passivation only affects the surface conditions opposite the low-temperature annealing, which affects the surface and the interface between the semiconductor and metal. In our study, we focused on very low annealing temperatures, below 100° C, to minimize thermal generation of bulk point defects that could act as recombination and trapping centers and negatively influence spectral resolution and charge-collection efficiency.

In the current study, we provide an insight into the influence of low-temperature annealing in ambient air at even lower temperatures (313–373 K), also covering in detail the temperature range of standard operation conditions of detectors (typically up to 333 K). One of the reasons for observed differences in impact of low-temperature annealing can be the influence of leakage currents flowing on the side surfaces of the sample. These currents strongly depend on the state of the surface, which varies with type of passivation and time. Therefore, we have utilized in this study a guard ring contact structure, which allowed for a separate structure separating bulk and surface leakage currents.

2. Experiment

The samples investigated in the study were the detector-grade materials CdTe:In and CdTe:Cl. Their fundamental properties are listed in table 1. The samples' resistivity was evaluated from I–V curves around 0 V after contact deposition. Gold and Indium were deposited on large opposite sides by evaporation. In this configuration, gold electrode blocks electrons and indium electrode blocks holes, while acting as cathode and anode, respectively. This polarity and high resistivity guarantee a low dark current. The assumed band bending of the Au/CdTe/In structure at 0 V, based on our previous analysis [10], is a negligible bending at the Au/CdTe and In/CdTe interfaces. The cathode contact was equipped with a guard ring to separate bulk and surface leakage currents during electrical measurements (figure 1). The surfaces were mechanically polished with Al_2O_3 abrasive (surface RMS 2 nm), without any further chemical treatment. The samples' n-type conductivity was determined by thermoelectric power measurements [11]. In CdTe:In, the measurement gave a clear signal which referred to n-type conductivity. The CdTe:Cl conductivity measurement had a weak n-type signal, which corresponds to a position of the Fermi level close to the midgap.

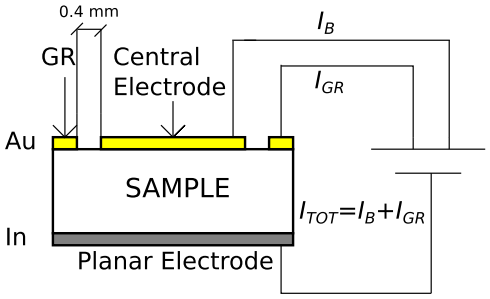

Figure 1. Measuring scheme for I–V characteristics.

The samples were annealed at temperatures 313–373 K with an annealing step of 10 K in ambient air. They were kept at each annealing temperature for 1 hour. Then the samples were cooled to room temperature, at which we performed I–V characteristic and ellipsometry measurements. Then they were heated up again to a temperature 10 K higher than the previous annealing temperature, and the whole cycle was repeated.

As the main research method, we used measurements of I–V characteristic evolution with annealing. We analyzed the bulk current and surface leakage currents separately. The Keithley 2410 sourcemeter was used to bias the samples. The bulk and leakage currents were measured on serial 1 MΩ resistors using two Keithley 6514 electrometers. To understand the origin of surface leakage currents, we investigated the side surfaces of the sample by ellipsometry after each annealing step. We measured the ellipsometry at room temperature immediately after cooling down from the annealing temperature.

We used a commercial JA Woollam Co. RC2 ellipsometer to measure the surface conditions and their development with increasing annealing temperature. The results were evaluated by a theoretical model published previously in [12]. The ellipsometry was measured in reflection mode with three incident angles of 55°, 60°, and 65°, respectively. The use of variable-angle spectroscopic ellipsometry was necessary to determine the surface-layer thickness. Acquisition time was 240 s and the range of spectral photon energies was between 1.24 and 4.00 eV. The incident light beam diameter was adjusted by an iris aperture to approximately 1.5 mm. The measurements were analyzed with CompleteEASE software. We applied models for CdTe, TeO_2, and Tellurium predefined in the Woollam database, which is supplied with the ellipsometer. This database contains predefined models for common materials, including CdTe and CdTe oxide. The CdTe material was parameterized by Lorentz oscillators and the CdTe oxide was parameterized with the Cauchy equation.

3. Results and discussion

The results of I–V measurements performed on the CdTe:Cl (−200 V, +200 V) and CdTe:In (−600 V, +600 V) samples at 300 K and different annealing temperatures are presented in figure 2. We separately show the bulk current I_B and the total current I_{TOT} that includes also the flow through the guard ring

Table 1. Basic properties of samples.

Sample	Dimension (mm^3)	ϱ (Ω cm)	Conductivity	Fermi Level (eV) [300 K]
CdTe:Cl	5.0 × 3.5 × 1.5	$\sim 10^{10}$	n-type	$E_c - 0.76$
CdTe:In	4.3 × 4.6 × 1.6	$\sim 10^{8}$	n-type	$E_c - 0.66$

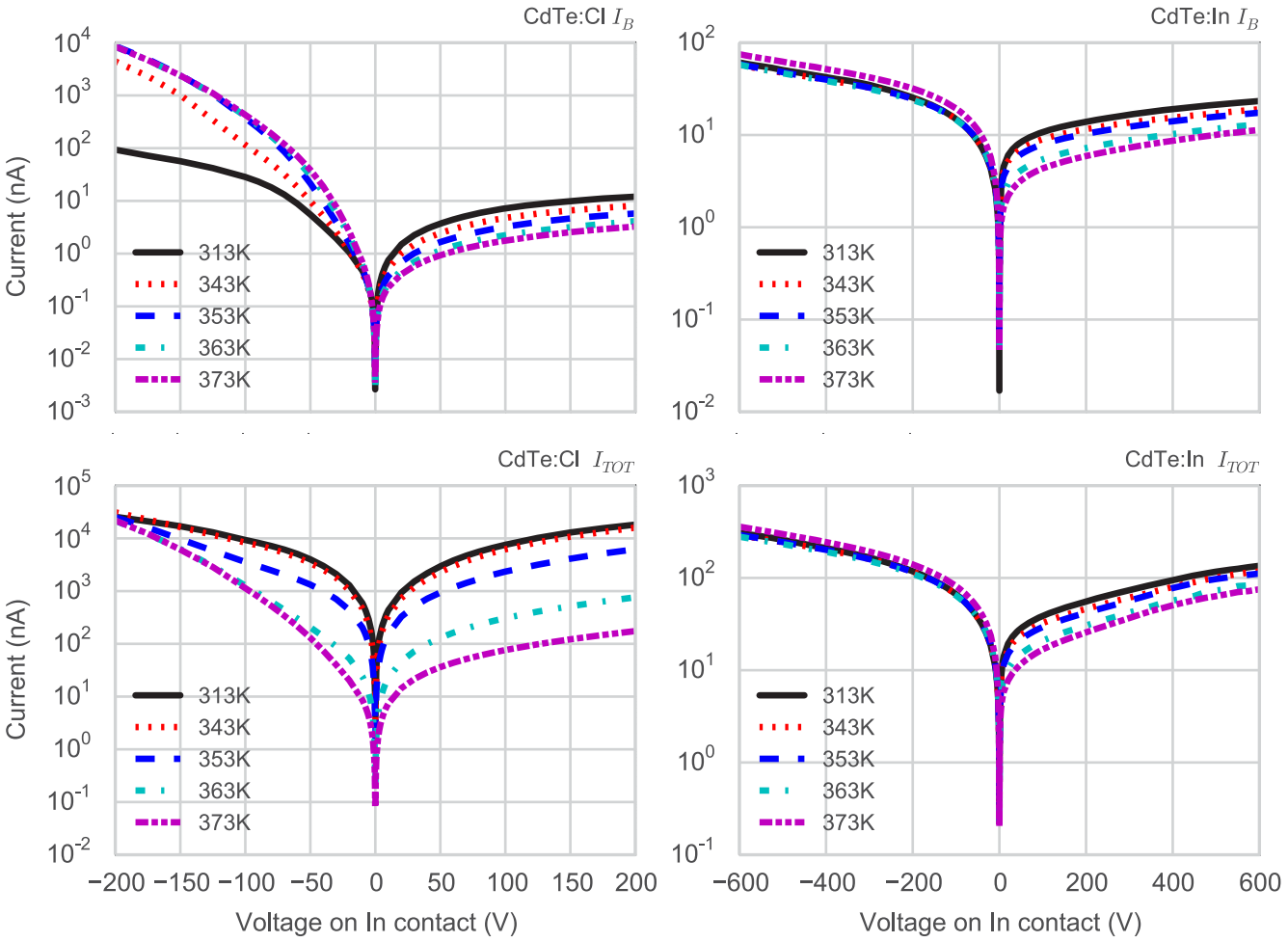

Figure 2. I–V characteristics of the bulk current I_B and the total current $I_{TOT} = I_B + I_{GR}$.

electrode and reflects the surface leakage current. The reason for the smaller measuring voltage range in the case of CdTe:Cl was the significant high current in the forward direction compared to CdTe:In (figure 2).

The bulk current in the reverse direction (In—anode, Au—cathode) decreased with the increasing annealing temperature. In the case of forward current, we observed an opposite effect whereby the bulk current increased with the increasing annealing temperature. In order to understand this effect we analyzed the I–V characteristics using an approach described in detail in [13].

We used a model that describes the dependence of the Schottky barrier height on the applied electric field [13]. The Schottky barrier height ϕ_{B0} decreased with an increased electric field in a reverse polarity, and the decline is described by the Schottky barrier lowering $\Delta\phi_B$. The I–V characteristics at high voltages in reverse direction are given by the equation

$$I_r = AA^*T^2 \exp\left(-\frac{(\phi_{B0} - \Delta\phi_B)}{kT}\right), \quad (1)$$

where A^* is the Richardson constant ($A^* = 12$ A/cm^{2}K^2 for CdTe), A is the area of the contact, k is the Boltzmann constant, and T is the absolute temperature. The simplest form of barrier lowering is due to the Schottky effect $\Delta\phi_B = e\sqrt{\frac{eE}{4\pi\varepsilon}}$, and the electric field is $E = \sqrt{\frac{2eN_t}{\varepsilon}U}$. Here, U is the applied bias, N_t is the deep-level concentration, e is the elementary charge, and ε is the absolute permittivity.

This model based on the Schottky barrier lowering is valid if the reverse current dependence $\ln(I)$ versus $U^{1/4}$ is linear.

The corresponding profiles of $\ln(I)$ versus $U^{1/4}$ for voltages in the range of 50–200 V for the CdTe:Cl sample and 50–600 V for the CdTe:In sample are presented in figure 3.

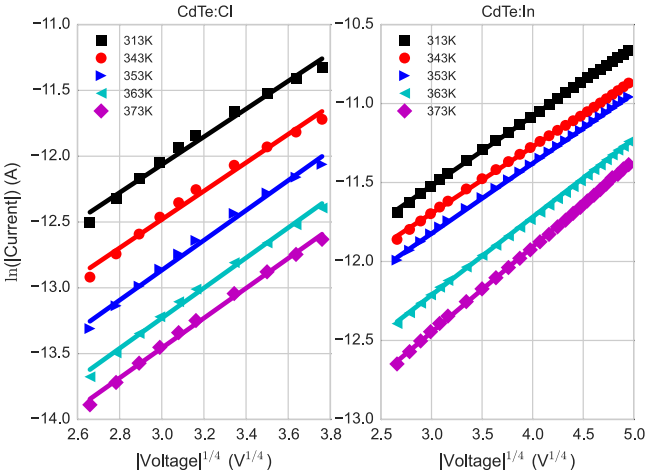

Figure 3. Dependence of $\ln(I)$ versus $U^{1/4}$ for the CdTe:Cl sample with annealing temperature as a parameter.

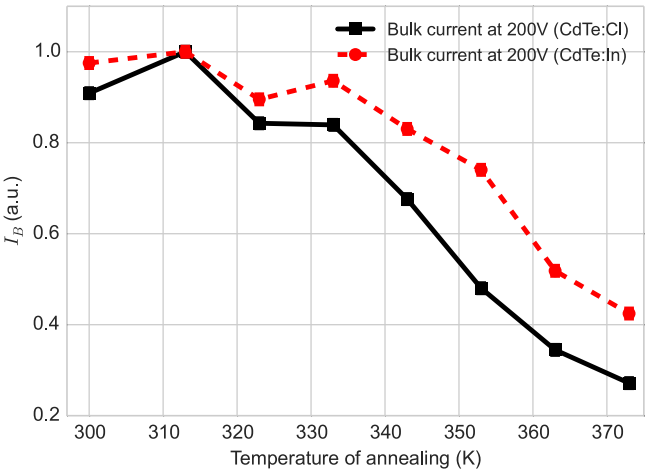

Figure 5. Normalized dependence of the bulk current on annealing temperature.

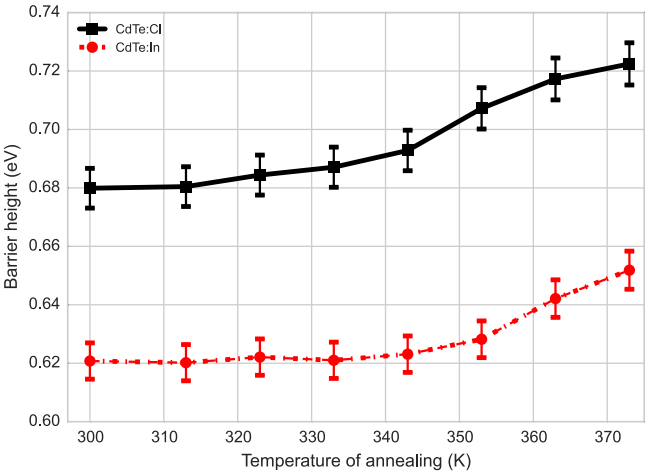

Figure 4. Dependence of the Schottky barrier height on annealing temperature.

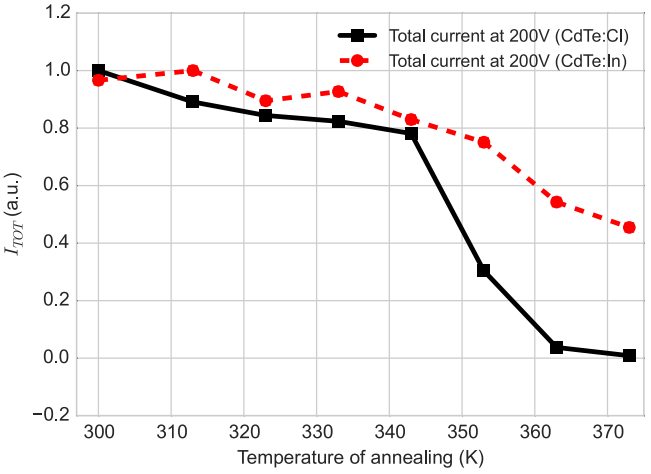

Figure 6. Normalized dependence of the total current on annealing temperature.

We evaluated the Schottky barrier height, limiting the current flow for both CdTe:Cl and CdTe:In samples, and the dependence of the annealing temperature is shown in figure 4. This figure also shows an increase of the Schottky barrier height with increasing temperature. The increase starts to be significant at annealing temperatures above 340 K, and is stronger for the CdTe:Cl sample. This concludes that the Schottky barrier increase is responsible for the observed reduction of the bulk current I_B (figure 5). The difference between the barrier height in the CdTe:Cl and CdTe:In as-grown samples approximately corresponds to the position of the Fermi level in these materials. Based on the n-type character of conductivity in both samples, we assume that the limiting Schottky barrier in the presented experiments is the Au/CdTe barrier (table 1). The Schottky barrier increase could be caused by diffusion of oxygen under the gold contact [7].

Let us now focus on the leakage current. It is apparent that in the reverse direction, the total current (figure 2) is almost entirely composed of the surface leakage current. Its dependence on the annealing temperature is for bias +200 V presented in figure 6. Because the total leakage current tends to critically depend on the surface conditions, we investigated the side-surface composition of the sample by ellipsometry after each annealing step.

Ellipsometric data were analyzed by a model consisting of the semi-infinite CdTe bulk layer, consisting of bulk CdTe, Te, and TeO_2 oxide and described by effective medium approximation (EMA), and the surface roughness layer. The EMA layer substitutes a non-uniform surface layer with material peaks and trenches with an average value, because the oxide layer grows on a rough non-uniform bulk surface [14, 15]. The results of the ellipsometric measurements are summarized in tables 2 and 3 for CdTe:In and CdTe:Cl, respectively. The tables also show the percentage distribution of Tellurium and TeO_2 in the EMA layer and the thickness of the EMA and surface roughness layers.

Figure 7 shows the dependence of leakage current I_{GR} at +200 V and the effective TeO_2 thickness in the surface layer on the sides of the CdTe:Cl (a) and CdTe:In (b) samples on annealing temperature. The effective TeO_2 thickness d_{TeO_2} is

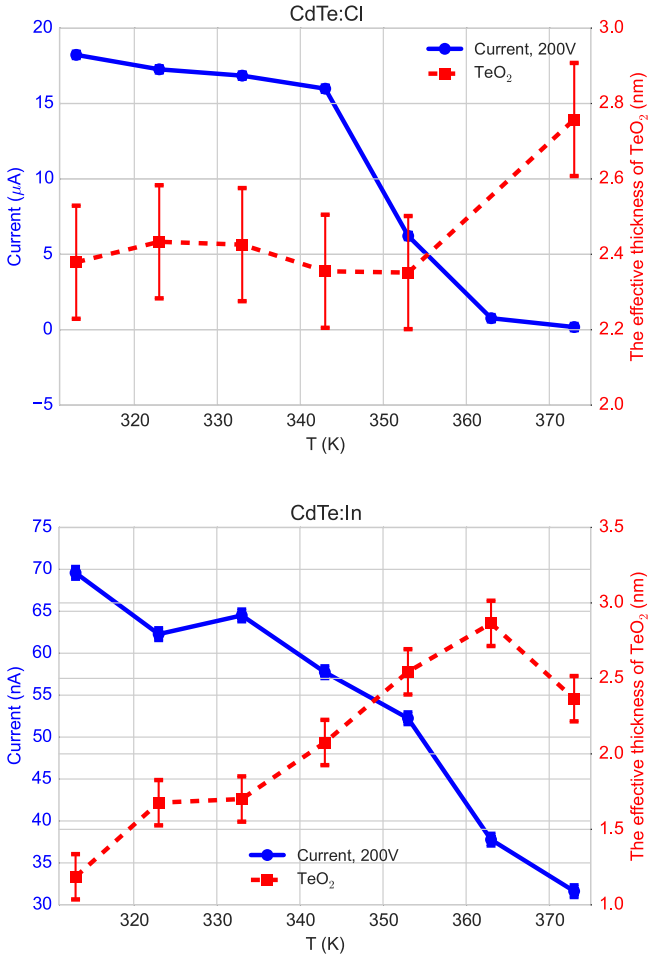

Figure 7. Room-temperature dependence of total current I_{TOT} at +200 V and the effective thickness of TeO_2 in the surface layer on sides of the CdTe:Cl and CdTe:In samples on annealing temperature.

Table 2. Results of ellipsometric data analysis for CdTe:In.

T (K)	Thickness (nm)	Tellurium (%)	TeO_2 (%)	Roughness (nm)
313	2.8	2.5	42.2	19.0
323	4.0	4.5	41.6	17.9
333	4.0	4.5	42.1	18.0
343	4.9	7.5	42.7	17.8
353	5.4	6.1	47.1	18.6
363	6.0	6.2	47.9	18.9
373	5.1	4.7	46.2	19.2

Table 3. Results of ellipsometric data analysis for CdTe:Cl.

T (K)	Thickness (nm)	Tellurium (%)	TeO_2 (%)	Roughness (nm)
313	2.8	0.0	65.9	9.1
323	4.0	0.0	63.2	9.3
333	4.0	1.7	61.1	9.4
343	4.9	8.1	57.3	10.0
353	5.4	9.4	55.2	10.4
373	4.7	5.0	58.3	10.6

described by

$$d_{TeO_2} = \frac{F_{TeO_2}}{100} d_{ST}, \tag{2}$$

where F_{TeO_2} is the TeO_2 filling factor and d_{ST} is the surface thickness. This TeO_2 effective thickness would correspond to the ellipsometry signal if the surface consisted of only a flat tellurium oxide layer. It is apparent that the leakage current and TeO_2 thickness are well anticorrelated. Therefore, the experimentally observed decrease of the leakage current can be associated with an increasing oxidation of the surface. We assume that the surface oxide layer modifies the surface leakage channels and/or results in depletion of the surface layer from majority carriers.

The elemental Te is located on the CdTe surface layer [3, 16, 17], and its change is caused by oxidation of the surface and evaporation of Cd. The elemental Te is oxidized into TeO_2 [14, 18], which causes a decrease of the Te filling factor in the surface layer. On the other hand, the evaporation of cadmium from the CdTe surface [17] increases the Te filing factor, and this is associated with the Te filling factor maximum at about 350 K. The increasing oxide layer causes the growth of the surface roughness.

We have estimated the Schottky barrier height error to about 1% due to temperature measurement error (about 0.1 K), current measurement error (1%), and error from the linear fit (figure 3). The TeO_2 thickness error, when examined by ellipsometry, was estimated to be 0.3 nm based on mathematical evaluation of mean-square error of the data fitting.

The presented results clearly show that low-temperature annealing at 300–373 K leads to a decrease of both the bulk and leakage currents. This effect is observed even at standard temperatures of detector operation (300–330 K) and accelerates at $T > 340$ K.

4. Conclusions

We have studied the influence of low-temperature annealing in ambient air on detector-grade CdTe:In and CdTe:Cl samples, especially the effect on their surface and bulk properties. We used annealing temperatures in the range where the CdTe detectors normally work. We measured the I–V characteristics and studied the sample surface composition by ellipsometry at room temperature after annealing. Both total current and bulk reverse current decrease after low-temperature annealing in CdTe samples. The total current behavior of the CdTe:Cl and CdTe:In samples agrees with the increase in the surface oxide layer thickness. The decrease of total current was more than 50% after the annealing. The evolution of the bulk current at reverse bias was related to the increase of the Schottky barrier height between metal and semiconductor after the annealing. The Schottky barrier increased from 0.62 to 0.65 eV between gold and CdTe:In, and from 0.68 to 0.72 eV in CdTe:Cl sample. This change had a significant influence on the reverse bulk current, which decreased by more than 50% of its initial value. We conclude

that low-temperature annealing can be used to improve metal–semiconductor interfaces.

Acknowledgments

This paper was financially supported by the Technological Agency of the Czech Republic under No. TE01020445 and grant SVV2017260445.

ORCID

M Rejhon https://orcid.org/0000-0001-7775-487X

References

[1] Horodyský P and Hlídek P 2006 *Phys. Status Solidi (b)* **243** 494–501
[2] Wang L, Sang W, Shi W, Qian Y, Min J, Liu D and Xia Y 2000 *Nucl. Instrum. Methods Phys. Res. Sect.* A **448** 581–5
[3] Wang X, Jie W, Li H, Li Q and Wang Z 2006 *Nucl. Instrum. Methods Phys. Res. Sect.* A **560** 409–12
[4] Chattopadhyay K, Ma X, Ndap J O, Burger A, Schlesinger T E, Greaves C M R, Glass H L, Flint J P, James R B and Schirato R C 2000 *Proc. Soc. Photo-Optical Instrum. Eng.* **4141** 303–8
[5] Ozaki T, Iwase Y, Takamura H and Ohmori M 1996 *Nucl. Instrum. Methods Phys. Res. Sect.* A **380** 141–4
[6] Park S, Ha J, Lee J, Kim H, Cho Y and Kim Y 2009-12-15 *J. Korean Phys. Soc.* **55** 2378
[7] Kim K H, Hwang S, Fochuk P, Nasi L, Zappettini A, Bolotnikov A E and James R B 2016 *IEEE Trans. Nucl. Sci.* **63** 2278–82
[8] Mergui S, Hage-Ali M, Koebel J and Siffert P 1992 *Nucl. Instrum. Methods Phys. Res. Sect.* A **322** 375–80
[9] Pekarek J, Belas E and Zazvorka J 2017 *J. Electron. Mater.* **46** 1996–2002
[10] Rejhon M, Franc J, Dědič V, Kunc J and Grill R 2016-09-21 *J. Phys. D: Appl. Phys.* **49** 375101
[11] Paez B 2000 *Phys. Status Solidi (b)* **220** 221–5
[12] Badano G, Million A, Canava B, Tran-Van P and Etcheberry A 2007 *J. Electron. Mater.* **36** 1077–84
[13] Sze S and Ng K K c 2007 *Physics of Semiconductor Devices* 3rd edn (Hoboken, N.J.: Wiley-Interscience) pp 136–9
[14] Zázvorka J, Franc J, Beran L, Moravec P, Pekárek J and Veis M 2016 *Science and Technology of Advanced Materials* **17** 792–8 pMID: 27933118
[15] Zázvorka J, Franc J, Statelov M, Pekárek J, Veis M, Moravec P and Mašek K 2016 *Appl. Surf. Sci.* **389** 1214–9
[16] Hirsch L S, Ziemer K S, Richards-Babb M R, Stinespring C D, Myers T H and Colin T 1998 *J. Electron. Mater.* **27** 651–6
[17] Häring J, Werthen J G, Bube R H, Gulbrandsen L, Jansen W and Luscher P 1983 *J. Vacuum Sci. Technol.* A **1** 1469–72
[18] Bahl M K, Watson R L and Irgolic K J 1977 *J. Chem. Phys.* **66** 5526–35